

Underactuation in robotic grasping hands

Thierry Laliberté[†], Lionel Birglen[†], and Clément M. Gosselin[†]

Abstract: This paper presents the development of selfadaptive and reconfigurable hands which are versatile and easy to control. These hands have three fingers and each of the fingers has three phalanges. The selfadaptability of the hands is obtained using underactuation. Also, the reconfigurability of the hands is obtained by reorienting the fingers. The design of a three-degree-of-freedom (dof) underactuated finger, used in all the hands, is first introduced. A first hand, which has 12 dofs and 6 motors is then presented. Subsequently, by including underactuation among the fingers and coupling their orientation, a second hand with 10 dofs and 2 motors is obtained. Finally, control issues and experimental results are presented.

Keywords: Grasping, hand, selfadaptive, underactuation.

1. Introduction

COMPLEX tasks involving the grasping of various objects in an unstructured environment are still being performed by human operators, even in hostile environments. One of the main obstacles to the teleoperation or automation of these tasks has been the lack of versatile grasping tools, i.e., of robotic hands. In many applications, the manipulation of objects with very complex mechanical hands [1][2][3] or human hands is often not essential and grasping devices are sufficient. However, simple grippers [4] are not appropriate in most cases because they are not capable of adapting to the shape of different objects. Hence, the development of versatile robotic hands which are capable of grasping a wide variety of objects with a very simple control structure is of great interest for many applications. Such hands can be obtained with the help of underactuation.

This paper presents underactuation in robotic grasping hands. First, the concept of underactuated grippers is introduced. Then, the design of three-dof fingers is discussed. Three of these fingers are then included in a hand having 6 motors. This hand is then modified in order to include underactuation among the fingers and obtain a hand with only 2 motors. Finally, control issues and experimental results are discussed.

2. Selfadaptation from underactuation

2.1 Underactuation

An underactuated mechanism is one which has fewer actuators than dofs. When applied to mechanical fingers, the concept of underactuation leads to selfadaptability. Selfadaptive fingers will envelope the objects to be grasped and automatically adapt to their shape with only one actuator and without complex control strategies. In order to obtain a determined system, elastic elements and mechanical limits must be introduced in statically underactuated mechanisms. While a finger is closing on an object, the

configuration of the finger at any time is determined by the external constraints associated with the object. When the object is fully grasped, the force applied at the actuator is distributed among the phalanges.

A closing sequence of an underactuated two-dof finger is shown in Fig. 1 in order to clearly illustrate the concept of underactuation. The finger is actuated through the lower link, as shown by the arrow in the figure. Since there are two dofs and one actuator, one (two minus one) elastic element must be used. In the present example, an extension spring is used which tends to maintain the finger fully extended. A mechanical limit is used to keep the phalanges aligned under the action of this spring when no external forces are applied on the phalanges. It should be noted that the sequence occurs with a continuous motion of the actuator. In *a*), the finger is in its initial configuration and no external forces are present. The finger behaves as a single rigid body in rotation about a fixed pivot. In *b*), the proximal phalanx makes contact with the object. In *c*), the second phalanx is moving with respect to the first one — the second phalanx is moving away from the mechanical limit — and the finger is closing on the object since the proximal phalanx is constrained by the object. During this phase, the actuator has to produce the force required to extend the spring. Finally, in *d*), both phalanges are in contact with the object and the finger has completed the shape adaptation phase. The actuator force is distributed among the two phalanges in contact with the object.

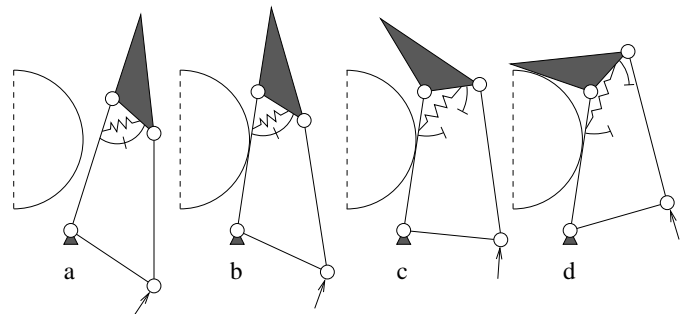


Fig. 1 Closing sequence of an underactuated two-dof finger.

* Received October XX, 2002; accepted Month XX, 2003.

[†] Department of Mechanical Engineering, Laval University, Ste-Foy QC G1K 7P4, Canada. E-mail: {thierry, birgle00, gosselin}@gmc.ulaval.ca

2.2 Literature review

A few underactuated fingers have been proposed in the literature. Some of them are based on linkages while others are based on tendon-actuated mechanisms. Examples of underactuated hands based on tendons are given in [5], [6] and [7]. Tendon systems are generally limited to rather small grasping forces and they lead to friction and elasticity. Hence, for applications in which large grasping forces are expected, linkage mechanisms are usually preferred and the present work is limited to the study of the latter mechanisms. One of the only studies on the statics of underactuated grippers is presented in [8]. In the latter reference, the static analysis of a system composed of two fingers, each having two dofs, is performed and some results are given to present the advantages of underactuated fingers over a simple parallel gripper. In [9], an underactuated hand with three fingers is presented. Each of the fingers is based on a two-dof mechanism having two phalanges and one actuator. Additionally, a special mechanism is introduced in order to allow the distal phalanges to be maintained orthogonal to the palm when precision grasps are performed. In [10], a mechanical hand resembling the human hand is presented. Each of the fingers is composed of three phalanges but has only two dofs since the motion of the last phalanx is directly coupled to the motion of the second phalanx. Another way to reduce the number of motors can also be found in the literature [11] [12]. It consists in using brakes or clutches in order to sequentially drive the different dofs with a single actuator. Such systems are different from the underactuated mechanisms described above in behaviour and implementation. It is also possible to reduce the number of motors by introducing compliance for each of the dofs. In [13], each of the fingers is linked to a common actuator through compliant springs. If one of the fingers is blocked, the other ones are not blocked for a certain range. The stiffness of the springs must be sufficiently small in order to allow adaptation. Therefore, the stiffness of the grasp is limited. Finally, it should be clearly understood that robotic or prosthetic fingers in which the motion is mechanically coupled [13] [14] [15] are not underactuated. Indeed, they are designed to mimic the motion of human fingers but the relative motion of the phalanges is determined at the design stage and therefore no shape adaptation is possible.

3. Stability of the grasp — equilibrium vs ejection

3.1 Static Analysis

Underactuation in robotic hands generates intriguing properties. For example, a finger cannot always apply forces with all its phalanges on the grasped object. To illustrate this point, consider the example of a 2-DOF underactuated finger that can be thought of as the last two phalanges of the prototypes presented below (Fig. 2).

In order to determine the configurations where this finger can apply forces to the object grasped, one shall proceed with a quasi-static modeling of the finger. The latter will provide us with the relationship between the input actuator torque and the forces exerted on the object. Equating the

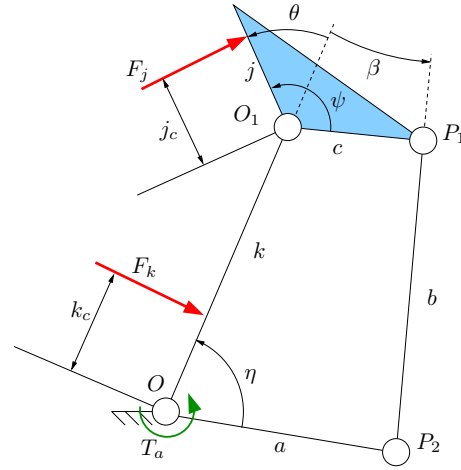


Fig. 2 Model of underactuated 2-DOF finger.

input and the output virtual powers, one obtains

$$\mathbf{t}^T \boldsymbol{\omega}_a = \mathbf{f}^T \mathbf{v} \quad (1)$$

where \mathbf{t} is the input torque vector exerted by the actuator and the spring, $\boldsymbol{\omega}_a$ is the corresponding velocity vector, \mathbf{f} is the vector of contact forces, and \mathbf{v} is the velocity of the contact points projected onto the respective normals of the phalanges. Contact forces are assumed to be normal to the phalanges and without friction. The projected velocities of the contact points can be simply expressed as the product of a Jacobian matrix \mathbf{J}_T and the derivatives of the phalanx joint coordinates which is a natural choice, i.e. $\mathbf{v} = \mathbf{J}_T \dot{\boldsymbol{\theta}}$. Through differential calculus, one can also relate vector $\boldsymbol{\omega}_a$ to the derivatives of the phalanx joint coordinates defined previously with an actuation Jacobian matrix \mathbf{J}_A , i.e. $\dot{\boldsymbol{\theta}} = \mathbf{J}_A \boldsymbol{\omega}_a$. Finally, one obtains

$$\mathbf{f} = \mathbf{J}_T^{-T} \mathbf{J}_A^{-T} \mathbf{t}, \quad (2)$$

which is the equation that provides a practical relationship between the actuator torques and contact forces. The resulting expression for \mathbf{f} has been verified with a classical static analysis. If the spring contribution is neglected — which is justified in practice — the analytical expressions are rather simple linear functions of the actuator torque, e.g. for the two-phalanx finger, one has

$$F_k = \frac{(j_c - h \cos \theta) k}{a k_c j_c (\cot \beta \cos \eta + \sin \eta)} T_a, \quad (3)$$

$$F_j = \frac{h}{a j_c (\cot \beta \cos \eta + \sin \eta)} T_a \quad (4)$$

where $h = c(\cos(\theta - \psi) - \sin(\theta - \psi) \cot \beta)$ is the distance between point O_1 and the intersection of lines (OO_1) and (P_1P_2) . Also, η is the angle between link a and the first phalanx. Moreover, if the springs are neglected, the phalanges are identical to a serial underactuated manipulator in the common sense of the term. Given the above result one can study the condition under which both F_k and F_j are positive, corresponding to a full-phalanx grasp, which is a function of the geometric configuration of the finger (described by vector $\boldsymbol{\theta}$) and the contact locations on the phalanges given by k_c and j_c . In an unstable configuration, the

closing process will force the finger to lose contact with the proximal phalanx. The distal phalanx contact is lost only in rare singular cases corresponding to hyperflexion of the finger. In such cases, contact is definitely lost, i.e. equilibrium cannot be attained anymore. In the other case, contact will only remain with the distal phalanx. However, an equilibrium position can still be attained but just for a one and unique particular position of contact j_c . Static analysis shows that this contact position should be

$$j_c = e = c \cos \theta (\cos(\theta - \psi) - \sin(\theta - \psi) \cot \beta) \quad (5)$$

with the corresponding contact force being

$$F_j = \frac{T_a}{a \cos \theta (\sin \eta + \cos \eta \cot \beta)}. \quad (6)$$

Note that the term $\cos \theta$ in the denominator of F_j also implies that contact can only be kept for $-\pi/2 < \theta < \pi/2$ which will be the boundaries of the graphs illustrating stability along with $0 < j_c < j$. It can be shown that the rest of the denominator of F_j is always positive. Geometrically, the above expression implies that the contact force should be located on the projection onto the distal phalanx of the intersection of lines (OO_1) and (P_1P_2) . Indeed, the distal phalanx is subjected to three pure forces, thus equilibrium can only exist if they all intersect in a common point. In previous work it has been conjectured that during the sliding of the phalanx along the contact point, the latter tends to converge towards the equilibrium point, which is, however, not always physically located on the phalanx, i.e. $\exists e \mid e > j$, which corresponds to situations that can lead to ejection. Unfortunately, this convergence does not always occur. To illustrate this point, examine the evolution of the contact location as seen from the phalanx. It can be easily shown that if only this contact exists and it is fixed in space, one has

$$j_c^2 - j_{ci}^2 + 2k(j_c \cos \theta - j_{ci} \cos \theta_i) = 0 \quad (7)$$

where j_{ci} and θ_i are an arbitrary initial configuration, for example, the instant when the contact on the first phalanx is lost. This equation allows us to obtain the precise evolution of the contact position with respect to the evolution of θ . The latter is itself determined by the location of the contact with respect to the equilibrium position. If the contact is located below the equilibrium point, the finger undergoes an opening motion and thus θ increases. Contact state evolves along the trajectories defined by eq. (7), and then, if the contact trajectory crosses the equilibrium equation defined by eq. (5), the grasp is finally stable, or else contact with the object will be lost, namely one obtains the ejection phenomenon (illustrated in Fig. 3). This phenomenon has been noticed in [16], [17], and is related to the self posture changeability of mechanisms described in [18], [19] but has never been closely studied despite its importance.

Depending on the geometric parameters of the mechanism, one can obtain the final stability of the grasp depending on the initial contact situation, as presented on Fig. 4 for a set of parameters presented in Table 1.

Contact trajectories defined above are indicated by dotted lines on Fig. 4, arrows indicate the direction of the contact evolution, and dashed lines indicate the equilibrium

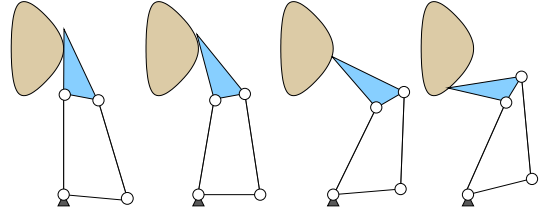


Fig. 3 The closing-ejection phenomenon.

Table 1 Geometric parameters

k	j	ψ	a	b	c
1	1/3	90°	1	6/5	1/3

equation. The contact state — defined by the pair (θ, j_c) — slides along a dotted line until either crossing the equilibrium curve (resulting in a stable grasp) or leaving the boundaries of the graph (contact lost, ejection). Given the evolution of θ , one can separate the equilibrium curve in two distinct stable parts, one attracting limit (the lower part on the graph) and a repulsive limit (upper part), the transition between the two modes being the tangent point between the contact trajectories and equilibrium curve, which is often close to the maximal ratio j_c/j theoretically attained by the equilibrium equation.

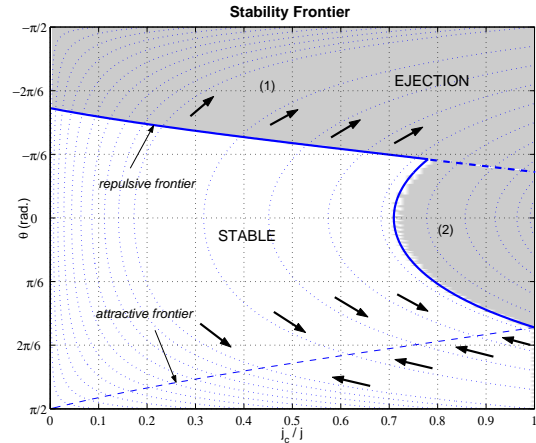


Fig. 4 Final stability of the grasp with one phalanx contact.

However, when the equilibrium point leaves physically the phalanx ($e > j$), another unstable frontier appears. Contact situations under the equilibrium curve and on the right hand side of the stability limit (shaded area number 2) are unstable because the contact trajectories cross the boundary $j_c/j = 1$ before attaining the attractive limit. The latter is not physically on the phalanx for this trajectory and this parameter set. This corresponds to the ejection phenomenon depicted on Fig. 3, ejection for a closing motion (θ increases) of the distal phalanx. Ejection for an opening motion (θ decreases) of the distal phalanx can also occur (shaded area number 1). If the distal phalanx tends to open, the motion of link a (thus motion as seen from the actuator) is still a closing process. Nevertheless, the contact situation will open the finger. This can and should be prevented using mechanical limits. For example, a mechanical limit such as $\theta > 0$ will eliminate the ejection of type 1 since the point of the contact trajectories with verti-

cal tangent are defined by

$$\begin{cases} \theta = 0 \\ j_c^2 - j_{ci}^2 + 2k(j_c - j_{ci} \cos \theta_i) = 0 \end{cases} \quad (8)$$

Furthermore, another limit such as $\theta < \pi/2$ should also be used since contact forces can only be kept for $-\pi/2 < \theta < \pi/2$ as discussed after eq. 6. The large regions of instability in Fig. 4 will hence be significantly reduced by using mechanical limits. One should also remember that unstable regions of type (1) on this figure corresponds to stable two-phalanx contact grasps. Each stability region is dual to the other. Hence, in most cases, i.e. when the contact is initially established with the proximal phalanx, the final grasp will be stable with the notable exception of the second type of unstable region. This type of instability should be therefore avoided as much as possible through suitable design. Moreover, if joint limits are used, they act as stable limits (however not attractive).

In conclusion, the equation of the equilibrium point is of utmost importance for the stability of the grasp and allows us to choose between two-phalanx (power) or one-phalanx (pinch) grasps. One shall then proceed with the detailed study of this function. These results can be extended to the three-phalanx case if there is no motion of the first phalanx or it is negligible.

3.2 Equilibrium Point Equation

The equilibrium equation (5) can be written as

$$e = c \cos \theta (\cos(\theta - \psi) - K \sin(\theta - \psi)) \quad (9)$$

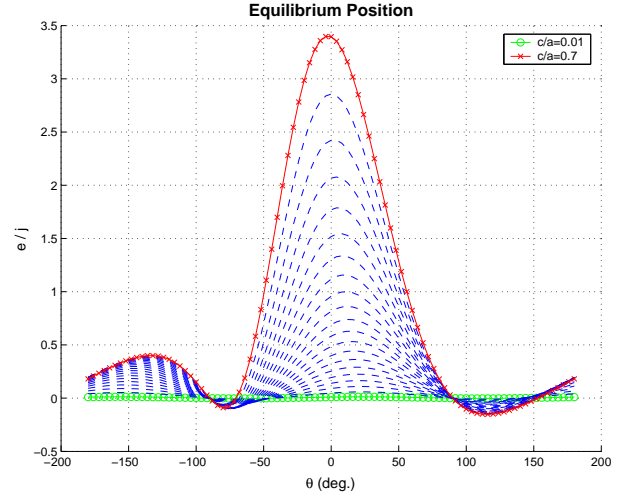
where $K = \cot \beta$ describes the opening of the four-bar linkage ($OO_1P_1P_2$). The equilibrium location equation (9) is primarily function of two parameters, namely the ratio c/a and the angle ψ . Their respective influence is shown in Fig. 5.

The limit ratio $c/a = 1$ (i.e. $\beta = 0$ in all configurations) should be avoided, since, in that case, the one-phalanx contact case is always unstable, due to the impossible equilibrium of the distal phalanx. The latter is subjected to three forces, two of them being always parallel. The equilibrium point is thus pushed to infinity. On the other hand, one can use the previous results to design a finger that eliminates the ejection phenomenon. One of these designs has been used in the prototypes presented in this paper.

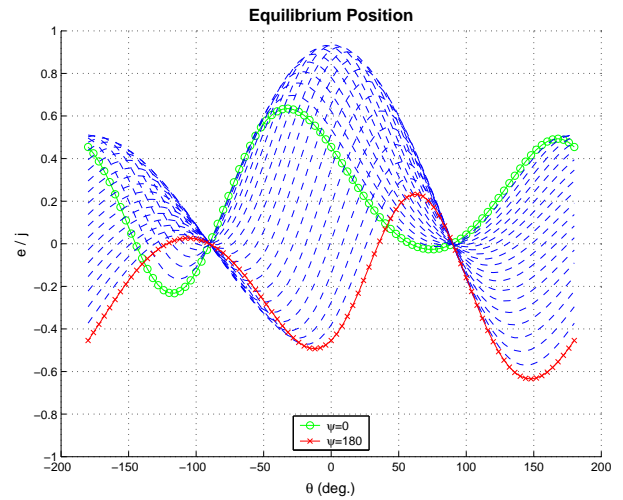
4. Three-dof underactuated finger

4.1 Design

As presented in the literature review, the existing underactuated fingers based on linkages have two phalanges or three coupled phalanges with two dofs. However, it is desirable to design an underactuated finger with three phalanges and three dofs since it leads to more stable grasps and more efficient shape adaptation. The result is a behaviour similar to that of human fingers. This finger mechanism has been introduced in [20] and is illustrated in Fig. 6. In order to obtain a three-dof finger with three phalanges, a four-bar mechanism is added to the five-bar mechanism of a two-dof finger. It is important to notice that the behaviour of the finger is determined by its geometry, prescribed at the design stage, since the different dofs cannot



(a) Influence of c/a



(b) Influence of ψ

Fig. 5 Equilibrium position.

be controlled independently. Hence, the choice of the design parameters is a crucial issue in order to obtain stable grasps and a proper distribution of the forces among the phalanges.

The different parameters involved in the design, illustrated in Fig. 6, are now discussed. The length of the phalanges, i.e., l , k , j are fixed from comparison with other existing fingers, simulations and experimentation with a finger model on objects to be grasped. The remaining design variables are a_i , b_i , c_i and ψ_i . In order to introduce design constraints and to reduce the number of independent variables, some relationships between these parameters are imposed, reducing the number of variables to two. In [16], it was shown that the behaviour of the fingers is mainly dictated by the ratios $R_i = a_i/c_i$. In order to minimize the 'thickness' of the finger, the length a_i should be as small as possible but is limited by mechanical interference considerations. Therefore, c_i is fixed, and then a_i is fixed for a given ratio. The performance of the finger regarding the stability of behaviour, the mechanical interferences and the internal forces is optimal if the transmission angle is close to 90

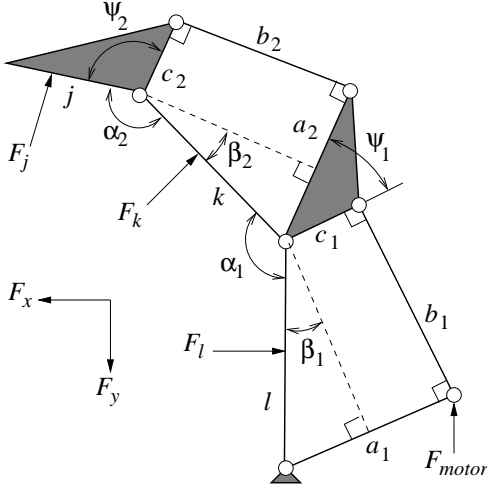


Fig. 6 Three-dof shape adaptation finger mechanism in an average configuration.

degrees when the finger is in an average configuration, as illustrated in Fig. 6. Note that the minimum and maximum values as well as the range of motion for the opening of each phalanx are the following (total ranges in parentheses): first joint, relative to the palm, 60 to 130 (70) degrees; second joint, $\alpha_1 = 90$ to 180 (90) degrees; and third joint, $\alpha_2 = 90$ to 200 (110) degrees. The parameters b_i and ψ_i can be computed from this criterion. First, the average configuration of the finger is defined as the configuration in which angles α_1 and α_2 are given by

$$\alpha_i = \frac{\alpha_{i,min} + \alpha_{i,max}}{2}, \quad i = 1, 2 \quad (10)$$

where $\alpha_{i,min}$ is the minimum value of angle α_i and $\alpha_{i,max}$ is its maximum value. Then, the average angles β_1 and β_2 , as defined in Fig. 6, are given by

$$\beta_1 = \arcsin\left(\frac{a_1 - c_1}{l}\right), \beta_2 = \arcsin\left(\frac{a_2 - c_2}{k}\right) \quad (11)$$

which leads to values of b_i given by

$$b_1 = l \cos \beta_1, \quad b_2 = k \cos \beta_2 \quad (12)$$

and to the values of ψ_i given by

$$\psi_1 = \pi - \alpha_1 + \beta_2 - \beta_1, \quad \psi_2 = \frac{3\pi}{2} - \alpha_2 - \beta_2 \quad (13)$$

Using the above equations as design constraints, all the geometric parameters can be computed as functions of the ratios R_1 and R_2 .

A study is then performed on fingers with different combinations of ratios R_i , giving an overview of possible fingers. To perform the study, a series of grasps are performed on circular objects (disks) of different sizes and at different positions relative to the palm, in order to simulate different sizes and shapes of objects, using a simulation tool presented in [16].

The main criteria used to determine the performance of the fingers are:

a) The sum of the forces applied by each finger on the object must be directed towards the palm (F_y) and the opposite finger (F_x) in order to obtain a stable grasp. Also, the

forces F_x should be larger than the forces F_y in order to obtain balanced grasps, since the forces F_y work in cooperation (towards the palm) and the forces F_x work in opposition (against each other). That is, $F_x = EF_y$, where the value of E depends on the type of grasp and is generally approximately equal to 2. The performance index associated with the resulting forces is given by the sum of the smallest force for each of the m objects grasped.

$$I_{xy} = \frac{\sum_{i=1}^m \min(F_{x,i}, EF_{y,i})}{m} \quad (14)$$

b) The forces should be well distributed among the phalanges in order to avoid large local forces on the object. The corresponding index is defined as the ratio of the total force on the three phalanges divided by the largest force.

$$I_{lkj} = \frac{\sum_{i=1}^m \frac{F_{l,i} + F_{k,i} + F_{j,i}}{\max(F_{l,i}, F_{k,i}, F_{j,i})}}{m} \quad (15)$$

c) An *equilibrium point* should exist on the last physical phalanx in all configurations in order to ensure feasible grasps and avoid object ejection, as discussed previously. If the equilibrium point is on the last physical phalanx, the index $I_{ep} = 1$; if it is not, the index $I_{ep} = 0$.

d) The finger mechanism should be as compact as possible. If the finger is sufficiently compact, the index $I_c = 1$. Otherwise, the index is between 0 and 1.

The performance indices are combined in order to obtain a global index

$$I_G = I_{xy}^2 I_{lkj} I_{ep} I_c \quad (16)$$

for each of the finger designs. The index I_{xy} is squared since it is the most important criterion. A graph of I_G as a function of R_1 and R_2 is presented in Fig. 7. An effective finger can then be chosen among the best values of I_G . For example, $R_1 = 2$ and $R_2 = 2.5$.

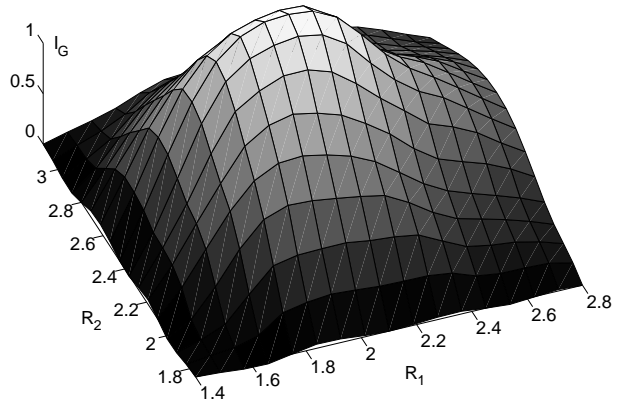


Fig. 7 Global performance index.

4.2 Parallel precision grasp mechanism

Underactuated fingers cannot perform precision grasps while maintaining the distal phalanges parallel to each other, for objects of different sizes. However, this feature allows more stable grasps when only the tips of the fingers are used and is very often feasible with simple grippers. A mechanism has been proposed in order to achieve this

behaviour for a two-dof underactuated finger [9]. A mechanism achieving a similar behaviour with the third phalanx of a three-dof underactuated finger has been developed here [20] and is illustrated in Fig. 8. It is composed of two parallelograms mounted in series. This mechanism is coupled to the phalanges of the finger but not to the other links of the shape adaptation mechanism (it is moving on a parallel plane). Two mechanical limits with springs at the top and bottom ends of the mechanism allow precision grasps to be performed and the adaptation to power grasps if necessary. This is illustrated in Fig. 8. In configurations (a), from dashed lines to full lines, a parallel motion of the distal phalanx is accomplished, by maintaining the parallelogram mechanism on its mechanical limits. In (b), a power grasp is performed, with contacts on all phalanges. In this case, the parallelogram mechanism is moved away from its mechanical limits and the distal phalanx is no longer maintained parallel.

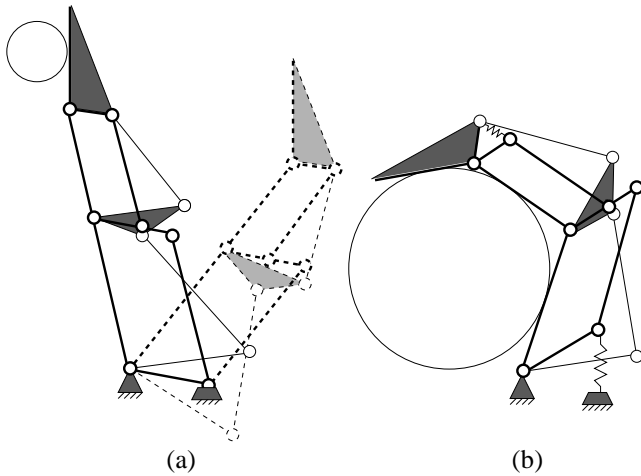


Fig. 8 The parallel precision grasp mechanism (dark lines). (a) parallel precision grasps. (b) power grasp.

4.3 Finger implementation

Three underactuated fingers identical to the finger described above are used in the design of selfadaptive robotic hands. The use of three fingers seems a good compromise for grasping since it is the minimum number of fingers required to accomplish stable grasps. Each of the three identical fingers is mounted on an additional revolute joint whose axis is located on the vertex of an equilateral triangle and oriented normal to the plane of the triangle. With these additional revolute joints, the hands can be reconfigured by modifying the orientation of the fingers in order to adapt to the general geometry of the object to be grasped. Note that this feature is widely used in the literature [9] [11] [21] in several different implementations. The main grasping configurations of the fingers are: cylindrical, spherical and planar. In the cylindrical configuration, two fingers point in the same direction while the third one points in the opposite direction and moves between the other two. In the spherical configuration, the three fingers are oriented towards the center of the triangle. In the planar configuration, two fingers are directly facing each other and the third finger is not used. The implementation of these configurations will be illustrated for each version of the hand.

The distance between the base of each of the fingers, or the size of the palm, raises issues which are similar to the ones considered when choosing the length ratios of the phalanges. A large palm allows the grasping of relatively large objects while a small palm allows the grasping of relatively small objects. Knowing the size of the objects to be grasped, the size of the palm can be determined by simulation. Also, the minimum and maximum size of the objects that can be grasped can be computed from geometric relationships.

5. Twelve DOF and six-degree-of-actuation (DOA) robotic grasping hand

This first hand has been built as a testbed in order to experiment the underactuated fingers and study grasping strategies. The surface of the fingers is flat since this is simple to machine and seems to be well suited to grasping. The tip of the fingers is not rounded — as it is often seen in other hands — in order to allow the grasping of small objects on a flat surface. The fingers have a total length of 16.5 cm from the first joint to the tip, and a width of 4 cm. The length of the phalanges are respectively, from base to tip: 7 cm, 5 cm and 4.5 cm. The distance from the centre to the vertices of the equilateral triangle is 6 cm. Each of the three fingers is mounted on an actuation module, as illustrated in Fig. 9. These modules are mounted on a mainframe and can be independently rotated. Each module comprises a main motor that drives the opening and closing of a finger. The transmission of the motor to the finger is composed of a ballscrew in order to obtain large forces, and a timing belt in order to obtain compact modules and allow the modification of the transmission ratio. Note that since a ballscrew is used, the fingers are backdrivable. Each module also comprises a small gearmotor to drive the orientation the finger. The transmission is performed via a gear attached to the motor and a gear attached to the mainframe. The three fingers can be rotated by 60 degrees, as illustrated in Fig. 10. Many configurations can be obtained, including the three main configurations previously introduced. Note that one of the fingers can be considered as a thumb as it is involved in all grasps.

Since each finger is driven by two motors, one for the grasping and one for the orientation, the hand has a total of six motors. Each finger has three grasping dofs and one orientation dof for a total of 12 dofs for the hand. The total mass of the hand is approximately 9 kg. The parts are made of aluminum, the shafts and screws are made of steel and the bushings are made of reinforced nylon. A CAD model and a picture of the complete hand is presented in Fig. 11.

6. Ten DOF and two DOA robotic grasping hand

In order to further reduce the number of actuators and hence further reduce the complexity of the controller, underactuation is now introduced not only into the fingers but also among them. Also, by keeping only the most useful finger orientations with respect to the base (Fig. 10), it is possible to couple the orientation of the fingers.

In addition to using the underactuated fingers, introducing underactuation among the fingers and coupling the orientation of the fingers leads to a robotic hand with ten dofs

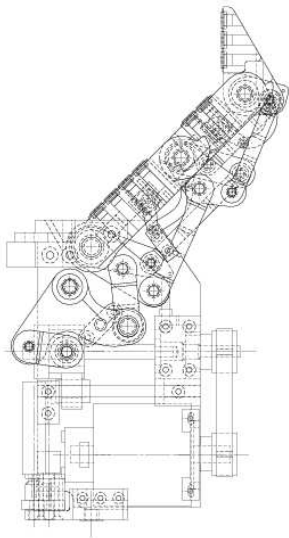


Fig. 9 A finger and actuation module.

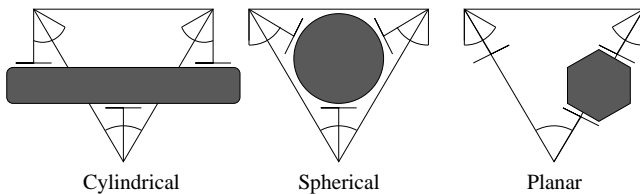


Fig. 10 Main configurations of fingers.

and two doas, illustrated in Fig. 12. One actuator is used to drive the underactuation system which controls the opening/closing of all three fingers via a transmission screw. The second actuator is used to drive the orientation of the fingers. To the best of the knowledge of the authors, this hand includes the combination of the underactuation of the phalanges of a finger and the fingers of a hand for the first time.

The prototype of this version of the hand has been designed to be mounted on the CART system at the Canadian Space Agency [22]. Therefore, it is scaled by a factor of 0.7 compared to the first version and its weight is 3.2 kg. The actuators are not included in finger modules but directly in the main frame.

6.1 Underactuation among the fingers

The application of the principle of underactuation among fingers has been demonstrated in the literature for the actuation of a few coupled-motion fingers [23] [21], each mechanism adding one degree of underactuation.

In the present hand, a one-input/three-output differential is used, adding two degrees of underactuation. Therefore, if some fingers are blocked, the remaining fingers will continue to close until they properly grasp the object. The force is fully applied only when all the fingers have properly made contact with the object or the palm. The overall system is illustrated in Fig. 13.

6.2 Reconfiguration

The main configurations of the fingers are obtained by orienting two of the fingers with a range of 90 degrees, as

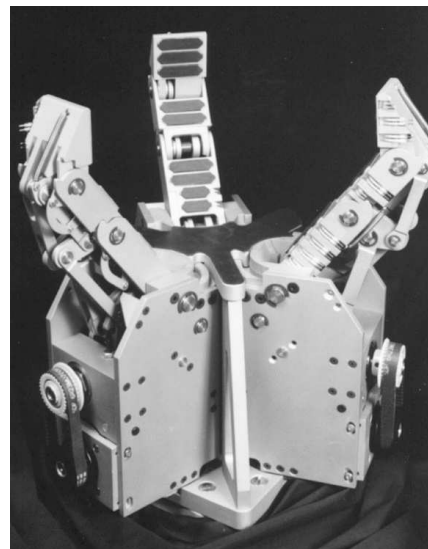
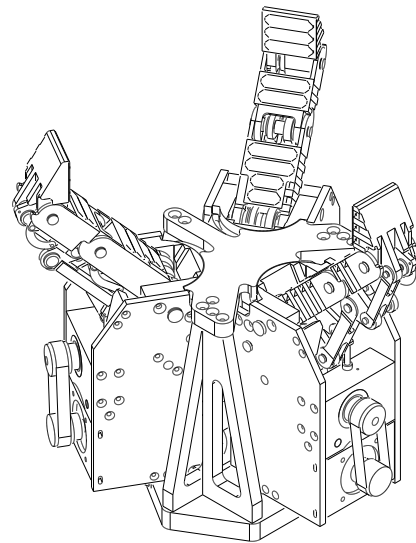


Fig. 11 CAD model and picture of the 12-dof 6-doa mechanical hand.

illustrated in Fig. 14. The rotation of the two fingers is coupled by a geared mechanism, shown in Fig. 15. In the planar configuration, where the third finger is not used, its closing is blocked at an output of the differential by a stopper activated by the orientation mechanism.

7. Control

7.1 General

Since there are fewer actuators than in a fully actuated hand, the control is simpler. Indeed, since properly designed underactuated mechanisms perform shape adaptation “automatically”, no motor coordination is needed.

Before performing a grasp, the geometry of the object should be determined and the hand should adjust itself to this geometry by orienting the fingers. To orient the fingers, a simple trajectory is generated to a prescribed position and the gearmotor follows this trajectory with a PD position control.

When the grasp is to be performed, a closing trajectory is generated up to a full closing position. The closing trajectory is followed using a PD position control loop. The position of the motors is obtained from optical encoders.

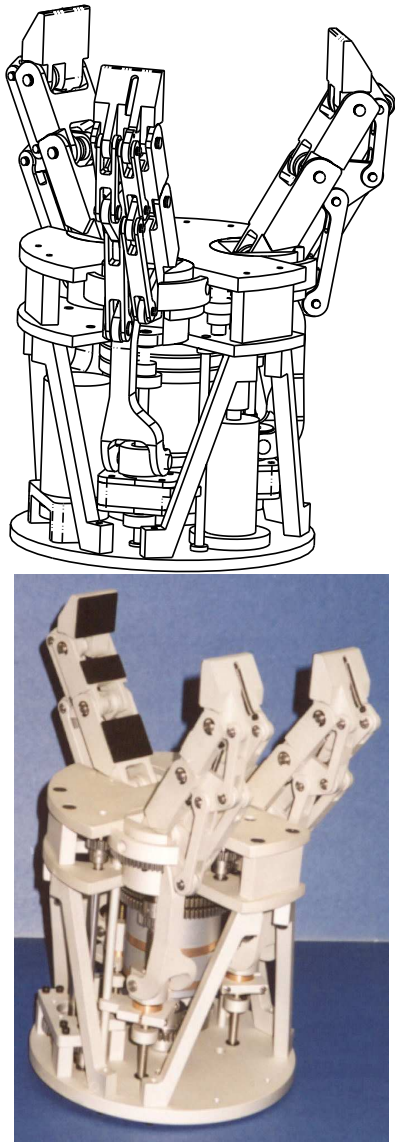


Fig. 12 CAD model and picture of the 10-dof 2-dof mechanical hand.

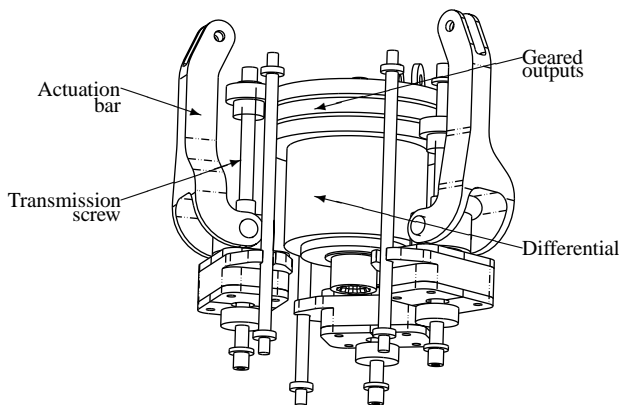


Fig. 13 One-input/three-output differential and transmission screws.

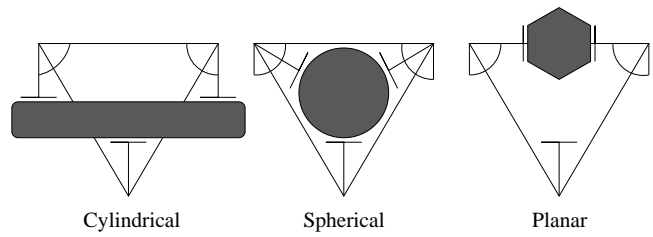


Fig. 14 Main configurations of fingers.

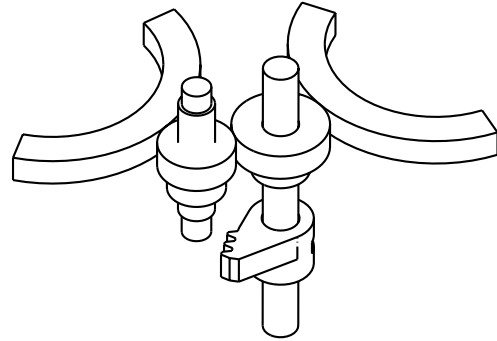


Fig. 15 The orientation mechanism. The two sections of gear are attached to the two orientable fingers. When appropriate, the teeth of the stopper will engage with one of the outputs of the differential.

In order to set the grasping force on the object, a maximum motor torque is set to a desired value. The relationship between the force on the object and the torque of the motor is obtained using the static model or by calibration. To set the maximum torque of the motor, it is assumed that the voltage is proportional to the current in the motor — which is true when the motor is stalled, which is generally the case when a grasp is performed — and that the current at the motor is proportional to the torque at the motor. When the grasp is performed, since the PD position control tries to reach full closing position, the force on the fingers corresponds to the maximum voltage set. The forces at the phalanges are not known accurately since no exact information on the configuration of the finger is used. The grasping force is therefore a coarse approximation, i.e., it can be considered light (30% of the maximum force), average (50%), large (70%) or very large (90%). This approximation is sufficient in most cases. Overall, the control strategy uses a closed-loop position control and an open-loop force control, which is very simple. With this control scheme, the grasping force is set and the resulting forces on the object is zero. If external forces are applied on the object they must be compensated. This compensation is implemented differently depending on the version of the hand and will be explained for each case.

If the hand loses the object, the fingers will suddenly close with a very large velocity since the fingers are very far from their prescribed position. This has two consequences: first, the loss of the object is immediately perceived and second, the high speed of the finger could damage the hand or the object. Therefore, the velocity of the finger should be limited to a given maximum speed. To do so, the voltage at the actuator is set to zero when the velocity exceeds the given limit. This will not stop the finger but will ensure that the

speed limit is not exceeded.

7.2 6-DOA hand

Since the hand is not fully underactuated, an interface has been developed to integrate the commands of each of the fingers. Each of the fingers can be controlled separately in position, velocity and force, but it is also possible to use the simple commands such as “close” and “open” for the whole hand. For the orientation, it is possible to prescribe a general orientation to each of the fingers independently, but it is also possible to prescribe directly the type of geometry of the grasp (spherical, cylindrical, planar) and the orientation of each of the fingers is automatically generated. The appropriate finger positions and relative forces will be set automatically depending on the orientation of the fingers. As an example for position control, for a planar grasp, the finger not involved in the grasp will not move. As an example for force control, the finger opposing the other two in the cylindrical grasp must be set to twice the force of the others. Therefore, when the “close” command is given, the hand behaves properly.

As noted previously, if external forces are applied on the grasped object, they must be compensated. The basic principle is to provide additional force to the fingers that are being pushed against by the external force and leave the force on the other fingers unchanged. To do so, an additional PD position control loop reacts only when a finger moves backwards from the initial grasping position. This PD control can be adjusted to yield a more or less stiff reaction to the external perturbations on the object.

In order to eventually develop and study fine force control, other sensors have been added. Two potentiometers are mounted in each of the fingers in order to measure the position of the second and third degrees of freedom of the fingers, giving the configuration of the fingers. Also, tactile sensors placed along the fingers, give the position of the contact points and provide some information on the force at these contacts.

7.3 2-DOA hand

Since there are only two motors, the control of the hand is simple and rather limited. No grasping coordination is needed by the control algorithm since the grasping of the fingers is mechanically coordinated by the differential, which tends to keep the forces on the fingers equal. If a grasp requires more force at one of the fingers, as in the cylindrical grasp, the finger will naturally compensate when pushed backwards because of the self-locking feature. The planar grasp is the only one that requires different finger positions and it is managed mechanically by the stopper previously described. No reconfiguration coordination is needed since the orientation of the fingers is coupled mechanically.

As noted previously, if external forces are applied on the grasped object, they must be compensated. Because of the transmission screws, the fingers are self-locking and they will naturally compensate external forces. Therefore, the simple initial control scheme can be used. In fact, since there is only one motor for the three fingers, the force at each finger cannot be controlled independently. Therefore,

the control algorithm modified for the 6 doa hand could not be used and self-locking is essential.

8. Experimentation

8.1 6-DOA hand

The hand has been tested on a GMF-S300 manipulator as illustrated in Fig. 16. The objective of the experimentation was to confirm the variety of shapes and sizes of objects which can be successfully grasped, the weight of the objects which can be grasped and the ability of the hand to grasp an object lying on a flat surface. Also, the characterization of the hand and the experimental validation of the control scheme was an important issue.

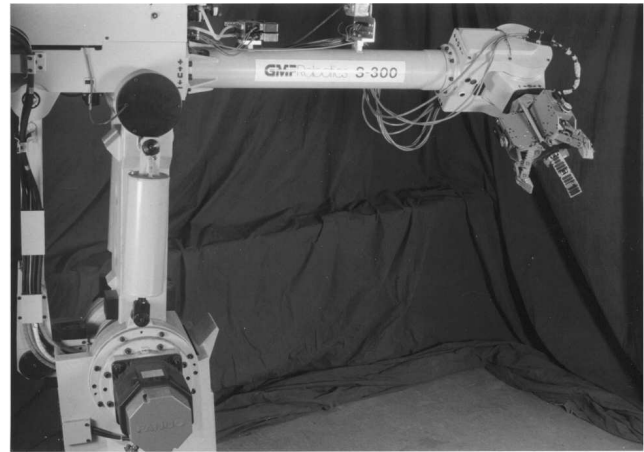


Fig. 16 The 6-doa hand mounted on the GMF-S300.

In order to test the adaptability of the hand, a wide range of objects have been grasped. The objects are first placed manually in the hand to show the ability to grasp virtually any object in many orientations. Then, the objects are grasped from a flat surface. Most of the objects have been successfully grasped, but with a limited number of types of grasp, e.g. pinch instead of power. The parallel pinch grasp has shown to be very useful in this situation. The smallest sphere grasped is a marble (1 cm diameter) and the largest is a volleyball (21 cm diameter). The smallest object grasped using a power grasp is a cylinder (2,5 cm diameter). Other objects grasped include a box, a chair, a disk, a tube, a boot, a baseball glove, a wooden bar, a screwdriver, a hammer, a barbell, a tennis ball, and a sheet of paper. In general, underactuated fingers performed surprisingly well. Examples of grasps are shown in Fig. 17. To test the power of the hand, heavier objects have been grasped and lifted. The ultimate test was to lift a person. The hand first grasps a steel bar and then a person was suspended from the steel bar. The combined weight was 155 lb (70 kg). Note that this mass is more than 7 times the mass of the hand itself. The mechanical structure of the hand has been designed to securely lift 200 lb (90 kg) in any orientation.

A special task was to use a first object (a tool) to lift a second object. An example was to grasp the hammer and to lift the chair with the hook of the hammer. Another special task was to grasp an electric screwdriver with two fingers and to use the third finger to push the button and activate the

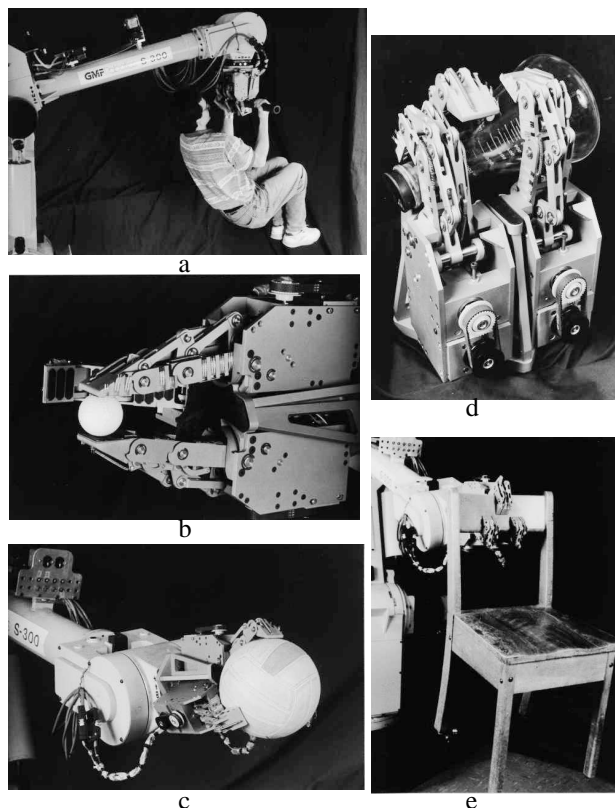


Fig. 17 Examples of grasps: a) person b) golf ball c) volleyball d) bottle e) chair.

screwdriver. This worked in two different configurations: in a power grasp and in a pinch grasp. The power grasp is more stable but the pinch grasp is more flexible, the axis of the screwdriver being normal to the palm.

The width of the fingers and the size of the hand may sometimes be cumbersome in constrained situations. For example, the handle of a suitcase is usually too small to be grasped with a power grasp and a different grasp must be used.

Experiments performed without the use of the tactile sensors tend to show that these sensors are not required in many grasping tasks. However, the hand could not grasp very fragile objects, such as an egg, and the information on the grasp is limited.

8.2 2-DOA hand

Some grasps, performed with a plastic version of the 2-DOA hand, are illustrated in Fig. 18. The possible grasps are essentially the same as with the 6-doa hand. The only task not possible was the grasp and activation of a screwdriver.

9. Conclusion

In this paper, different prototypes of underactuated mechanical hands have been presented. It is shown that underactuated hands can effectively perform a variety of grasps with very simple control algorithms. The version with 6 doas requires some simple motor coordination while the version with 2 doas requires only minimum control algorithms — similarly to simple grippers — and has grasping capabilities comparable to the version with 6 doas. Future work includes the study of more refined control using

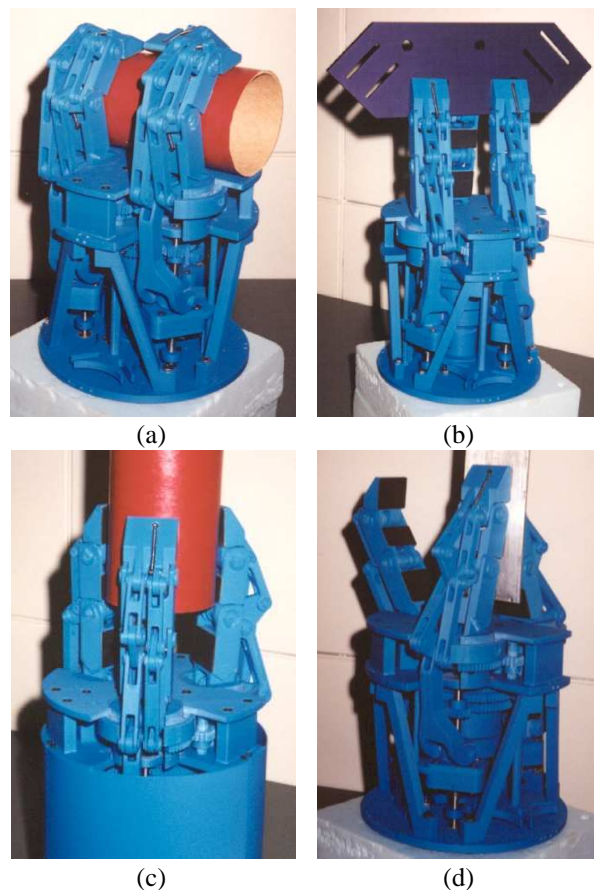


Fig. 18 Examples of grasps with SARAH P1: (a) Cylindrical power grasp. (b) Cylindrical precision grasp. (c) Spherical precision grasp. (d) Planar precision grasp, note that one of the fingers is blocked open to allow an effective grasp.

additional sensors, such as tactile sensors and the investigation of other implementations of underactuation.

Acknowledgements

The work reported here was performed under research grants from the Institut de Recherche en Santé et Sécurité du Travail (IRSST), the Natural Sciences and Engineering Research of Canada (NSERC) and MDRobotics. Funding was also provided by the Canada Research Chair on Robotics and Mechatronics currently held by Clément Gosselin.

References

- [1] S.C. Jacobsen, J.E. Wood, D.F. Knutti, and K.B. Biggers, "The UTAH/M.I.T. Dextrous Hand: Work in Progress," *The International Journal of Robotics Research*, Vol. 3, No. 4, pp. 21–50, 1984.
- [2] M.T. Mason, J.K. Salisbury, *Robot Hands and the Mechanics of Manipulation*, The MIT Press, Cambridge, 1985.
- [3] J. Butterfass, M. Grebenstein, H. Liu and G. Hirzinger, "DLR-Hand II: Next Generation of a Dextrous Robot Hand," *Proceedings of the International Conference on Robotics and Automation*, Seoul, South Korea, pp. 109–114, 2001.
- [4] F.Y. Chen, "Gripping Mechanisms for Industrial Robots: An Overview," *Mechanism and Machine Theory*, Vol. 17, No. 5, pp. 299–311, 1982.
- [5] J.D. Crisman, C. Kanojia and I. Zeid, "Graspar : A Flexible, Easily Controllable Robotic Hand," *IEEE Robotics and Automation Magazine*, pp. 32–38, June 1996.
- [6] D.F. Graham, "Artificial Hand and Digit Therefor," U.S. Patent 5 200 679, 1993.
- [7] S. Hirose and Y. Umetani, "The Development of Soft Gripper for

- the Versatile Robot Hand," *Mechanism and Machine Theory*, Vol. 13, pp. 351–359, 1978.
- [8] H. Shimojima, K. Yamamoto and K. Kawawita, "A Study of Grippers with Multiple Degrees of Mobility," *JSME International Journal*, Vol. 30, No. 261, pp. 515–522, 1987.
- [9] S.J. Bartholet, "Reconfigurable End Effector," U.S. Patent 5 108 140, 1992.
- [10] R.M. Crowder and D.R. Whatley, "Robotic Gripping Device Having Linkage Actuated Finger Sections," U.S. Patent 4 834 443, 1989.
- [11] N. Ulrich and V. Kumar, "Grasping Using Fingers with Coupled Joints," *Proceedings of the ASME Mechanisms Conference*, Vol. 15-3, pp. 201–207, 1988.
- [12] S. Lee, "Artificial Dexterous Hand," U.S. Patent 4 946 380, 1990.
- [13] N. Dechev, W.L. Cleghorn and S. Naumann, "Multiple Finger, Passive Adaptive Grasp Prosthetic Hand," *Mechanism and Machine Theory*, Vol. 36, No. 10, pp. 1157–1173, 2001.
- [14] J. Zhang, G. Guo and W.A. Gruver, "Optimal Design of a Six-Bar Linkage for an Anthropomorphic Three-Jointed Finger Mechanism," *Proceedings of the ASME Mechanisms Conference*, Phoenix, vol. DE-45, pp. 299–304, 1992.
- [15] E.N. Haulin, A.A. Lakis and R. Vinet, "Optimal Synthesis of a Planar Four-Link Mechanism Used in a Hand Prosthesis," *Mechanism and Machine Theory*, Vol. 36, Nos. 11–12, pp. 1203–1214, 2001.
- [16] T. Laliberté and C.M. Gosselin, "Simulation and Design of Underactuated Mechanical Hands," *Mechanism and Machine Theory*, Vol. 33, No. 1/2, pp. 39–57, 1998.
- [17] S. Montambault and C. M. Gosselin, "Analysis of Underactuated Mechanical Grippers," *ASME Journal of Mechanical Design*, vol. 123, no. 3, pp. 367–374, 2001.
- [18] M. Kaneko and T. Hayashi, "Standing-up Characteristic of Contact Force During Self-posture Changing Motions," *Proceedings of the IEEE International Conference on Robotics and Automation*, pp. 202–208, 1993.
- [19] M. Kaneko and K. Tanie, "Contact Point Detection for Grasping of an Unknown Object Using Self-posture Changeability (SPC)," *Proceedings of the IEEE International Conference on Robotics and Automation*, pp. 864–869, 1993.
- [20] C.M. Gosselin and T. Laliberté, "Underactuated Mechanical Finger with Return Actuation," U.S. Patent 5 762 390, 1998.
- [21] G. Guo, X. Qian and W.A. Gruver, "A Single-DOF Multi-Function Prosthetic Hand Mechanism With an Automatically Variable Speed Transmission," *Proceedings of the ASME Mechanisms Conference*, Phoenix, vol. DE-45, pp. 149–154, 1992.
- [22] J.C. Biedboeuf and É. Dupuis, "Recent Canadian Activities in Space Automation and Robotics - An Overview," Section 3.7, *Proceedings of the 6th I-SAIRAS*, St-Hubert, Canada, June 2001.
- [23] M. Rakik, "Multifingered Robot Hand with Selfadaptability," *Robotics and Computer-Integrated Manufacturing*, Vol. 5, No. 2-3, pp. 269–276, 1989.
- Canada, in 1985, at which time he was presented with the Gold Medal of the Governor General of Canada. He then completed a Ph.D. at McGill University, Montréal, Québec, Canada and received the D. W. Ambridge Award from McGill for the best thesis of the year in Physical Sciences and Engineering in 1988. In 1988 he accepted a post-doctoral fellowship from the French government in order to pursue work at INRIA in Sophia-Antipolis, France for a year. In 1989 he was appointed by the Department of Mechanical Engineering at Université Laval, Québec where he is now a Full Professor since 1997. He is currently holding a Canada Research Chair on Robotics and Mechatronics since January 2001. He also received, in 1993, the I. Ω. Smith award from the Canadian Society of Mechanical Engineering, for creative engineering. In 1995, he received a fellowship from the Alexander von Humboldt foundation which allowed him to spend 6 months as a visiting researcher in the *Institut für Getriebetechnik und Maschinendynamik* of the *Technische Hochschule* in Aachen, Germany. In 1996, he spent 3 months at the University of Victoria, for which he received a fellowship from the BC Advanced Systems Institute.
- His research interests are kinematics, dynamics and control of robotic mechanical systems with a particular emphasis on the mechanics of grasping and the kinematics and dynamics of parallel manipulators and complex mechanisms. His work in the aforementioned areas has been the subject of several publications in International Conferences and Journals. He is a member of the Institute for Robotics and Intelligent Systems (IRIS), one of the networks of the Canadian Centres of Excellence and he is the French language editor for the International Journal *Mechanism and Machine Theory*.
- Dr. Gosselin is a member of ASME, IEEE, and CCToMM.

Biographies

Thierry Laliberté received the B.Eng. degree in Mechanical Engineering from Université Laval in 1992 and the Master's degree in Mechanical Engineering from Université Laval in 1994. He has been awarded a post-graduate scholarship by the Natural Sciences and Engineering Research Council of Canada (NSERC). He is currently a research engineer in the Robotics Laboratory of the Mechanical Engineering Department at Université Laval. His research interests are selfadaptive grippers, static balancing, path planning and rapid prototyping of mechanisms.

Lionel Birglen received the B.Eng. degree in Mechatronics from École Nationale Supérieure des Arts et Industries de Strasbourg, France, in 2000. He is currently pursuing a Ph.D. degree in Mechanical Engineering within the Robotics Laboratory at Université Laval, after an accelerated promotion from M.Sc. His work focuses on the kinematic analysis and control of complex mechanical hands and parallel manipulators, with a particular emphasis on force control and general theory of real-time control. Lionel Birglen is a student member of IEEE and ASME.

Clément M. Gosselin received the B.Eng. degree in Mechanical Engineering from the Université de Sherbrooke, Québec,